

PUBLISHED VERSION

Boinepalli, Sharada; Attard, Phil.

Grand canonical molecular dynamics, *Journal of Chemical Physics*, 2003; 119(24):12769-12775.

© 2003 American Institute of Physics. This article may be downloaded for personal use only. Any other use requires prior permission of the author and the American Institute of Physics.

The following article appeared in *J. Chem. Phys.* **119**, 12769 (2003) and may be found at <http://link.aip.org/link/doi/10.1063/1.1629079>

PERMISSIONS

http://www.aip.org/pubservs/web_posting_guidelines.html

The American Institute of Physics (AIP) grants to the author(s) of papers submitted to or published in one of the AIP journals or AIP Conference Proceedings the right to post and update the article on the Internet with the following specifications.

On the authors' and employers' webpages:

- There are no format restrictions; files prepared and/or formatted by AIP or its vendors (e.g., the PDF, PostScript, or HTML article files published in the online journals and proceedings) may be used for this purpose. If a fee is charged for any use, AIP permission must be obtained.
- An appropriate copyright notice must be included along with the full citation for the published paper and a Web link to AIP's official online version of the abstract.

31st March 2011

<http://hdl.handle.net/2440/55397>

Grand canonical molecular dynamics

Sharada Boinepalli

CSSM, University of Adelaide, SA 5005 Australia

Phil Attard

School of Chemistry F11, University of Sydney, NSW 2006 Australia

(Received 27 August 2003; accepted 1 October 2003)

A hybrid molecular dynamics-Monte Carlo grand canonical simulation technique is developed for systems with constant chemical potential and temperature. The method ensures that the particle number and energy fluctuate according to the standard grand canonical probability distribution. Partial coupling and fractional particles are used to enhance the success of insertion and deletion attempts, and the method is shown to be feasible in dense liquids. The method is applied to a Lennard-Jones fluid and it gives the density as a function of chemical potential in agreement with known results. It is demonstrated that the transport coefficients can be obtained with the method by analyzing the influence of the stochastic perturbation on the diffusion constant for an isothermal system. © 2003 American Institute of Physics. [DOI: 10.1063/1.1629079]

I. INTRODUCTION

The behavior of solids, liquids or gases can be simulated at the molecular level in two ways, viz., molecular dynamics and Monte Carlo methods. Molecular dynamics, which uses a deterministic approach, gives information about the time evolution of a system. On the other hand, Monte Carlo methods are stochastic in nature and are useful in understanding the system in equilibrium. Conventionally molecular dynamics methods are used for systems with constant N (number of particles), volume V , energy E and more recently with fixed N , V , and temperature T . Molecular dynamics techniques were not favored to study open systems with changing number of particles. Such grand canonical (GC) systems were studied mainly using Monte Carlo (MC) techniques. This is because the insertions and deletions of particles needed in such studies fit nicely with the MC's stochastic moves, but they are not easily incorporated into Hamilton's equations of motion in a molecular dynamics calculation. As a result, time dependent properties such as transport coefficients, or liquid vapor condensation which might be best studied in the GC ensemble in, for example, confined geometries, are studied by the NVT -MD. Therefore a necessary bridge between MD and GCMC is a molecular dynamics simulation of a grand canonical system, known as GCMD. Such a scheme would have an advantage over GCMC in computing dynamical properties, and an advantage over NVT -MD in, e.g., confined fluids.

Previous grand canonical molecular dynamics schemes may be divided into deterministic extended system approaches¹⁻³ and schemes with a stochastic contribution and separated MD and GCMC volumes.⁴⁻⁷ In the former the particle number is a continuous variable whose fractional part is related to the strength of the solute coupling parameter and which evolves deterministically in time according to certain equations of motion. In the latter exchange by diffusion occurs between the MD volume, in which the particles

obey Hamilton's equations, and the stochastic volume, in which GCMC moves are employed.

The scheme that we propose here is also a type of stochastic MD, with the random GC moves occurring in the same volume as the deterministic steps of the MD trajectory. Like the extended system approaches, particle number is a continuous variable with the fractional part representing the solute-solvent coupling; in the present case it evolves stochastically. Hence instead of inserting or deleting full particles, as in crude GCMC, we intend to grow or shrink the particles gradually via the fractional coupling. The aim and motivation for the present technique is that the trajectory followed should reproduce the equilibrium grand canonical probability distribution.

The present method is an extension of the hybrid technique proposed by Attard⁸ for isothermal simulations. That method is very similar to an earlier hybrid method developed by Anderson.⁹ In these methods deterministic time steps using Newton's equations are alternated with stochastic steps depending upon the Boltzmann distribution. The methods yield the standard canonical distribution.

Our new method extends the hybrid technique for temperature control to chemical potential control of a system in contact with a reservoir. Such a stochastic approach to study molecular dynamics has many advantages. Since the controlling pseudopotential in the Boltzmann factor used in this method is derived from the probability distribution of a grand canonical system, it guarantees the correct probability distribution, and system averages are simple unweighted averages over the trajectory. The simple GC algorithm equilibrates the system faster than the standard MD approach. Once equilibrium has been attained dynamical properties can be calculated. The stochastic control can be easily controlled with parameters that represent the strength of the kick to the momentum and fractional particle coupling. By keeping the strength of the kick to the fractional particle small, we can

ensure that the particles change slowly and without effecting the dynamics drastically.

This paper aims to prove that dynamical properties can be studied with the stochastic molecular dynamics method and goes on to derive a methodology for stochastic molecular dynamics of a grand canonical system, and test the methodology. A Lennard-Jones (LJ) grand canonical system in contact with a reservoir at fixed chemical potential μ and temperature T is simulated and its equilibrium density is noted. The computer simulations are repeated for different chemical potential and the equilibrium densities are compared with those in the literature.

II. A COMBINED MC AND MD TECHNIQUE FOR GRAND CANONICAL SIMULATIONS

A. Equations of motion

The model describes a system of N_{total} particles that can exchange particles and energy with a reservoir at fixed temperature and chemical potential. Here the particle number N_{total} is a continuously varying real number instead of being an integer. The total number of particles in the system at any instant is the sum of an integer and a fractional part, $N + \xi$, N being the number of full particles and ξ , a fractional part with weight ξ . The forces on the particles in the system are mainly due to the interparticle potentials and an effective reservoir force. The particles in the system evolve according to the equations of motion,

$$\dot{q}_{i\alpha} = \frac{\partial \mathcal{H}^{\text{total}}}{\partial p_{i\alpha}} = \frac{p_{i\alpha}}{m}, \quad (1)$$

$$\dot{p}_{i\alpha} = -\frac{\partial \mathcal{H}^{\text{total}}}{\partial q_{i\alpha}} = F_{i\alpha} + f_{i\alpha}, \quad (2)$$

where i labels the atom and α labels the coordinate. The total energy of the reservoir and system is represented by the Hamiltonian $\mathcal{H}^{\text{total}}$. The force felt by a particle labeled i due to the other particles in the system is $F_{i\alpha}$ and the effective force exerted on the particle by the reservoir is denoted by $f_{i\alpha}$.

The total Hamiltonian of the system with N particles and an $N+1$ st fractional particle with weight ξ consists of the kinetic energy and one- and two-body potentials. It can be written as

$$\begin{aligned} \mathcal{H}^{\text{total}} = & \sum_{i=1}^N \frac{p_i^2}{2m} + \sum_{i=1}^{N-1} \sum_{j=i+1}^N U_{ij} + \sum_{i=1}^N u_i + \frac{p_{N+1}^2}{2m} \\ & + \sum_{i=1}^N U_{i(N+1)}(\xi). \end{aligned} \quad (3)$$

The summation variable and subscript i indicate the full particles and the subscript $N+1$ indicates the fractional particle. The deterministic force F , is the spatial derivative of the summed pairwise potential due to the particles in the system, U and the stochastic force is the spatial derivative of the potential due to the reservoir u , which is not required explicitly. The potential energy of the system due to the fractional particle is coupled through ξ . The kinetic energy coupling is taken to be independent of ξ in the current paper. The deter-

ministic force decides the time evolution of the existing particles in the system according to Hamilton's equations. At the end of the deterministic time step, Δt_d , the positions and momenta of the N particles and the fractional particle are computed according to

$$q_i(t + \Delta t_d) = q_i(t) + \Delta t_d \frac{p_i(t)}{m}, \quad (4)$$

$$p_i(t + \Delta t_d) = p_i(t) + \Delta t_d F_i(t), \quad (5)$$

and for the $(N+1)$ st fractional particle,

$$q_{N+1}(t + \Delta t_d) = q_{N+1}(t) + \Delta t_d \frac{p_{N+1}(t)}{m}, \quad (6)$$

$$p_{N+1}(t + \Delta t_d) = p_{N+1}(t) + \Delta t_d F_{N+1}(t). \quad (7)$$

The forces are given explicitly in the next section.

The stochastic force, on the other hand, changes the momentum and the number of particles in a random fashion and hence needs two separate types of moves. These will be modelled using the Metropolis algorithm. The simulation of every time interval contains two steps, a deterministic step followed by a stochastic step. Physical parameters of interest like the potential energy, the kinetic energy, and pressure are completed at the end of the total time step, to be used in the next cycle.

B. Pseudopotential for a grand canonical system

The Metropolis algorithm attempts to move the system through various randomly chosen configurations and accepts or rejects them depending on the pseudopotential that appears in the Boltzmann factor. The pseudopotential for a system that changes its number of particles as it evolves from one configuration to another is derived below.

The unconditional transition probability for a system going from a configuration Γ at time t to Γ' at time $t + \Delta t$ is defined by

$$M(\Gamma'; \Gamma) = \tau(\Gamma'; \Gamma) P(\Gamma), \quad (8)$$

where $\tau(\Gamma'; \Gamma)$ is the conditional probability and $P(\Gamma)$ is the probability that the system is in state Γ . To ensure that the probability is stationary we require that the transition probability be reversible, that is

$$M(\Gamma'; \Gamma) = M(\Gamma; \Gamma'). \quad (9)$$

While this condition is not physically correct, it does ensure stationarity,¹⁰ and it is sufficient for the present equilibrium purposes.

In the Metropolis algorithm a new configuration is randomly chosen and an attempt is made to move the system to it. The move is accepted or rejected according to the change in a certain factor. Hence the transition probability from a state Γ to another Γ' depends on the probability $M_{\text{trial}}(\Gamma'; \Gamma)$ of choosing the particular state Γ' and the probability of it being accepted. The probability of choosing the configuration Γ' obeys a similar equation to $M(\Gamma'; \Gamma)$, i.e.,

$$M_{\text{trial}}(\Gamma'; \Gamma) = \tau_{\text{trial}}(\Gamma'; \Gamma) P(\Gamma). \quad (10)$$

The attempt to move from Γ to Γ' is accepted if the inequality

$$\frac{M_{\text{trial}}(\Gamma; \Gamma')}{M_{\text{trial}}(\Gamma'; \Gamma)} > \kappa \quad (11)$$

(where κ is a random number uniformly distributed on $[0,1]$) holds good. If the ratio is smaller than κ , the move to the new configuration is rejected. This ensures that $M(\Gamma'; \Gamma)$ is symmetric even if $M_{\text{trial}}(\Gamma'; \Gamma)$ is not. Hence for the grand canonical system under consideration we define the change in pseudopotential from the above ratio.

For a grand canonical system of N particles with energy \mathcal{H}_N and chemical potential μ , the probability density is given by

$$\wp(\Gamma | \mu, V, T) = \frac{e^{\beta\mu N - \beta\mathcal{H}_N}}{N! h^{3N} Z(\mu, V, T)}, \quad (12)$$

where $Z(\mu, V, T)$ is the grand canonical partition function and $\beta = 1/k_B T$, where k_B and T are Boltzmann's constant and temperature, respectively.

Let P_c be the trial probability of a creation attempt into the system in configuration Γ^N . At this stage we consider only whole particles; the result for the fractional particles will be given at the end of the section. The transition rule for creation due to which the system goes from configuration Γ^N to Γ'^{N+1} is chosen to be

$$\tau_{\text{trial}}(\Gamma'^{N+1}; \Gamma^N) = \frac{P_c P_{\text{MB}}(p'_{N+1}) \delta(\Gamma'^N - \Gamma^N)}{V}. \quad (13)$$

The new particle created is assigned coordinates randomly in the volume V , hence the trial probability is proportional to $1/V$. The momentum for the new particle is taken from the Maxwell Boltzmann distribution given by

$$P_{\text{MB}}(p) = \Lambda^3 h^{-3} \exp(-p^2/2mk_B T), \quad (14)$$

Λ and h being the thermal wavelength and Planck's constant, respectively. The delta function ensures that the configuration of the original N particles remains unchanged.

The corresponding rule for deletion of the N th particle is

$$\tau_{\text{trial}}(\Gamma'^{dN-1}; \Gamma^N) = P_d \delta(\Gamma'^{N-1} - \Gamma^{N-1}), \quad (15)$$

where $P_d = 1 - P_c$, is the probability of a deletion attempt.

For the Metropolis algorithm, we need a pseudopotential to be used in the form of $\exp(-\beta w_c)$. For attempts of creation this will be, using Eq. (11),

$$e^{-\beta w_c} = \frac{\tau_{\text{trial}}(\Gamma^N; \Gamma'^{N+1}) \wp(\Gamma'^{N+1})}{\tau_{\text{trial}}(\Gamma'^{N+1}; \Gamma^N) \wp(\Gamma^N)}. \quad (16)$$

Using Eqs. (12)–(14), this will yield

$$\begin{aligned} e^{-\beta w_c} &= \frac{P_d V e^{\beta\mu} e^{-\beta(\mathcal{H}_{N+1} - \mathcal{H}_N)}}{P_c \Lambda^3 h^{-3} e^{-\beta p_{N+1}'^2/2m} (N+1) h^3} \\ &= \frac{P_d V e^{\beta\mu} e^{-\beta(U_{N+1} - U_N)}}{P_c \Lambda^3 (N+1)}. \end{aligned} \quad (17)$$

Notice that the kinetic energy dependence has disappeared. This is because we decided to sample the new particle's momentum from a Maxwell–Boltzmann distribution. A similar calculation for deletion attempt yields

$$e^{-\beta w_d} = \frac{P_c N e^{-\beta\mu} e^{-\beta(U_{N-1} - U_N)}}{P_d \Lambda^{-3} V}. \quad (18)$$

Choosing $P_d = P_c$, for creation we get

$$\begin{aligned} e^{-\beta w_c} &= \frac{(V\Lambda^{-3})^{N+1} N! e^{\beta\mu(N+1)} e^{-\beta U_{N+1}}}{(V\Lambda^{-3})^N (N+1)! e^{\beta\mu N} e^{-\beta U_N}} \\ &= e^{-\beta(w(N_{\text{new}}) - w(N_{\text{old}}))}, \end{aligned} \quad (19)$$

where $w(N)$ is the pseudopotential given as

$$w(N) = Nk_B T \ln N - Nk_B T - Nk_B T \ln(V\Lambda^{-3}) - N\mu + U_N. \quad (20)$$

The calculation for deletion yields the same pseudopotential. Considering N as a continuous number of the form $N + \xi$, a change in pseudopotential at every time step can be evaluated as

$$\Delta w = w(N_{\text{new}}) - w(N_{\text{old}}). \quad (21)$$

The variable number N is a continuous, real number rather than an integer. This makes the pseudopotential a continuous function. A change in particle number corresponds to ξ_{old} going to ξ_{new} . When $\xi_{\text{new}} > 1$, a new fractional particle is created with coupling $\xi_{\text{new}} - 1$, and the old fractional particle is now a full particle. When $\xi_{\text{new}} < 0$, the current fractional particle is deleted and one of the full particles is made the new fractional particle with coupling $1 + \xi_{\text{new}}$. When $0 < \xi_{\text{new}} < 1$, no particles are created or destroyed and only the strength of the coupling of the current fractional particle is changed.

The volume factor that appears in the pseudopotential has previously been used in GCMC calculations, but the justification for it is the asymmetry of M_{trial} for creation and destruction and not rescaling of coordinates as might have been assumed.

III. SIMULATION METHOD

The simulation starts with N_{total} particles being assigned spatial coordinates in a cubic box of volume V and velocities from a Maxwell–Boltzmann distribution at temperature T . One of the particles is randomly identified as the fractional particle of weight $\xi = 1$ to begin with.

The interparticle potential for full particles is the LJ potential given as

$$U_{ij} = 4\epsilon \left[\left(\frac{\sigma}{q_{ij}} \right)^{12} - \left(\frac{\sigma}{q_{ij}} \right)^6 \right], \quad (22)$$

where ϵ is the well depth of the potential and σ is the diameter of the i th and j th particles separated by a distance q_{ij} .

The deterministic time step computes new positions and velocities for all the particles, depending on the forces on individual particle according to Eqs. (4)–(7). The deterministic force between the i th and j th particle is the spatial derivative of the LJ potential,

$$F_{ij} = - \frac{\partial U_{ij}}{\partial q_{ij}}. \quad (23)$$

The fractional particle couples to the potential energy of the system via its weight ξ . The potential energy felt by the fractional particle due to the i th full particle is given by

$$U_{i\xi} = 4\epsilon_{\xi} \left[\left(\frac{\sigma_{\xi}}{q_{i\xi}} \right)^{12} - \left(\frac{\sigma_{\xi}}{q_{i\xi}} \right)^6 \right]. \quad (24)$$

A nonlinear coupling is used to couple the fractional particle into the system. We have used the coupling scheme given by Kaminsky¹¹ according to which the potential well depth and diameter for the fractional particle are related to its weight through $\epsilon_{\xi} = \xi^{1/3}\epsilon$ and $\sigma_{\xi} = \xi^{1/4}\sigma$, where ϵ and σ are the well depth and diameter of full LJ particles. The coupling through a slowly varying parameter ξ ensures that the potential energy is a slowly varying function and changes continuously with particle number $N + \xi$.

Shroll and Smith,³ in an extended system GCMD study of SPC water, included a bias potential for the solute coupling to improve sampling efficiency. It would of course be relatively easy to implement umbrella sampling in the stochastic phase of the present GCMD technique. In the present LJ study we found the nonlinear coupling scheme of Kaminsky¹¹ to be very efficient and no umbrella sampling¹² or force bias¹³ was required.

The second part of the time step is the stochastic perturbation which attempts to give a random kick to the momenta of all the particles and the fractional particle ξ . Left to itself the temperature of the system would tend to rise, mainly due to the limited accuracy of the molecular dynamics algorithms. Traditionally this is countered by scaling the velocities of all the particles at regular intervals and maintaining the equilibrium temperature. We attempted a stochastic method to control the temperature as described in Attard.⁸ This models one of the effects of the stochastic force of the reservoir. The stochastic move ensures that phase space points are visited with the correct Boltzmann weight. Hence GC system averages are simple unweighted averages over the trajectory.

A. Stochastic temperature control

The first stochastic move aims to model the effect of the random force due to the reservoir on the momenta. A cycle is made through all the atoms treating each component of their momentum in turn. At each stage, the trial move gives a random kick to the momentum component of one of the particles. The trial move gives a random kick to momenta of all the particles and a decision is made as to reject or accept this move depending on the kinetic energy Boltzmann factor. The change in momentum of an i th particle in α direction is given by

$$p_{i\alpha}^{\text{trial}} = p_{i\alpha}(t + \Delta t_d) + \Delta p, \quad (25)$$

where $\Delta p = \Delta_i f_{i\alpha}$, Δ_i is a random number uniformly distributed in $[-p^*, p^*]$, and $p_{i\alpha}(t + \Delta t_d)$ is the momentum of the i th particle at the end of the deterministic time step. The move is accepted or rejected according to the kinetic energy Boltzmann factor. The change in energy due to the trial move is

$$\Delta \mathcal{H} = [(p_{i\alpha}^{\text{trial}})^2 - p_{i\alpha}^2(t + \Delta t_d)]/2m. \quad (26)$$

The trial change is accepted unconditionally if the change in kinetic energy is negative. On the other hand if the change is positive, it is accepted with a probability of $\exp(-\beta\Delta\mathcal{H})$. A random number κ , uniformly distributed on $[0,1]$ is sampled and the move is accepted if and only if,

$$\exp(-\beta\Delta\mathcal{H}) \geq \kappa. \quad (27)$$

Stochastic temperature control depends very much on the choice of the value for p^* which is here taken to be

$$p^* = \lambda \sqrt{mk_B T}, \quad (28)$$

where λ is generally of the order of 0.01.

B. Stochastic chemical potential control

The other effect of the stochastic force, $f_{i\alpha}$ on the system causes a change in the number of particles in the system. The system tries to attain equilibrium with the reservoir at a fixed chemical potential. The second trial move attempts to change ξ by giving it a random kick, i.e., $\xi^{\text{trial}} = \xi(t + \Delta_d) + \Delta_{\xi}$, where Δ_{ξ} is chosen from an interval $[-\xi^*, \xi^*]$. ξ^* is of the order of 0.1. The acceptance or rejection of the trial move is in accord with the pseudopotential given by Eq. (20). If the change in pseudopotential is negative, it is accepted unconditionally and if it is positive, it is accepted with a probability $e^{-\beta\Delta w}$.

At every simulation step an attempt is made to change ξ by a small amount $\Delta\xi$. If the changed ξ is greater than 1, the current fractional particle has become a full particle. The remaining part of the new ξ is assigned to another new fractional particle as $\xi' = \xi - 1$. The newly created fractional particle is assigned position coordinates in the volume V , and velocities from a Maxwell–Boltzmann distribution. If the changed ξ is less than 0, the current fractional particle is removed from the system. A new fractional particle is selected and the remaining part of the negative ξ is assigned to it as $\xi' = 1 + \xi$. This ensures the continuous evolution of ξ . If the changed ξ lies between 0 and 1, the fractional particle has simply changed in its size and coupling.

After deciding upon the new configuration, the change in pseudo-potential, Δw is computed as in Eq. (20). The trial configuration is accepted unconditionally if Δw is negative. If it is positive, a uniformly distributed random number κ is sampled and the configuration is accepted if and only if,

$$\exp(-\beta\Delta w) \geq \kappa. \quad (29)$$

C. Tail correction

The interparticle LJ potential between pairwise particles is cutoff and hence a tail correction is needed in the physical quantities like potential energy, pressure, chemical potential. We included the tail correction as a separate term in the pseudopotential to be calculated at every time step as

$$u_{\text{tail}}(\xi) = \epsilon_{\xi} \rho^* \left[\frac{16\pi\sigma_{\xi}^{12}}{9r_c^9} - \frac{16\pi\sigma_{\xi}^6}{3r_c^3} \right], \quad (30)$$

where r_c is the cut-off length, ϵ_ξ and σ_ξ are the potential well depth and particle diameter respectively, for the fractional particle. It is computed at every step using the instantaneous density at that time, ρ^* .

With tail correction the pseudopotential becomes

$$w(N) = Nk_B T \ln N - Nk_B T - k_B T \ln(V\Lambda^{-3}) - N\mu + U_N^{\text{cut}} + \tilde{u}_{\text{tail}}(\xi). \quad (31)$$

Here U_N^{cut} is the sum of LJ pair potentials cut-off at r_c . In practice, only those pair potentials that are affected by the change in ξ need be computed (including any fractional particles made full or deleted). The tail correction is

$$\tilde{u}_{\text{tail}}(\xi) = \begin{cases} u_{\text{tail}}(\xi + 1) - u_{\text{tail}}(1), & \xi < 0 \\ u_{\text{tail}}(\xi), & 0 \leq \xi \leq 1 \\ u_{\text{tail}}(\xi - 1) + u_{\text{tail}}(1), & \xi > 1. \end{cases} \quad (32)$$

The extra terms account for the change in pair potentials in U_N upon deletion or creation events. The effect of the tail correction on equilibrium densities is discussed with the results in the following sections.

IV. RESULTS

A. Stochastic temperature control

We simulated a system with fixed number of particles, ($N=125$) in a cubic box, for the stochastic temperature control part. The size and volume of the box depend on the density under simulation. We ran cases with different temperature, density combinations and examined the kinetic energy and diffusion during the entire run. Hamilton's equations of motion were solved with the simplest scheme, to first order of time step, which we took initially at 10^{-4} . (The unit of time is $\sqrt{m\sigma^2/\epsilon}$.) In principle, higher order of time steps and more sophisticated schemes can be used to solve the equations of motion.

All the physical variables are rendered dimensionless using well depth ϵ , diameter of full LJ particles σ and mass m .

The system was observed for 10 000 time steps after equilibration. The efficiency of the thermostat to maintain the equilibrium temperature depends very much on the choice of λ , which measures the strength of the push to the momentum. We did simulations with different values of λ to arrive at an optimum value for good temperature control of the system. The kinetic energy variation for the system with density and temperature as $\rho^*=0.9535$ and $T^*=2.69$ is shown in Figs. 1 and 2.

The profile of the kinetic energy during the simulation with values of $\lambda=0.01$ and 0.05 shows that the higher value of λ controls the temperature better (see Figs. 1 and 2). However, the insufficient temperature control with a lower λ can be improved by improving the efficiency of the molecular dynamics algorithm. Due to the reasons explained below, we chose the lower value of 0.01 for λ , which meant an inferior thermostat, and we reduced the Δt_d to 10^{-5} to improve the efficiency of the algorithm. But a lower time step results in too many kicks to the momentum in the stochastic step. So we reduced the frequency of the momentum kicks to only once in every ten time steps. Typically acceptance rates for λ

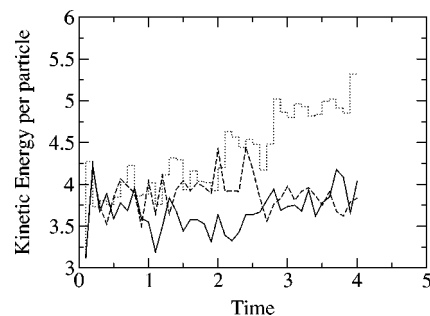


FIG. 1. Kinetic energy per particle variation during simulation with $\lambda=0.01$. The dotted line has a time step of 10^{-4} , the dashed line has a time step of 10^{-5} , and the solid curve has a time step of 10^{-5} , but the stochastic change to momentum is applied only once in every ten time steps. Here $\rho^*=0.9535$ and $T^*=2.69$. The expected kinetic energy per particle of the system is 1.5 times T^* which is 4.03.

values 0.01 and 0.05 are 99% and 98%, respectively. As can be seen from the solid curves in Fig. 1, this gives adequate temperature control.

Diffusion is one process that reflects the dynamics of the particles in the system. We examined the diffusion of the system to understand if the dynamics of the system were being effected by the stochastic thermostat used to control the temperature. This is done by computing the diffusion coefficient.

For a system with N particles, diffusion coefficient can be calculated by computing the distance travelled by each particle from its original position. At any time t diffusion coefficient $D(t)$ is given by

$$D(t) = \frac{\sum_{i=1}^N (q_i(t) - q_i(0))^2}{6tN}, \quad (33)$$

where $q_i(t)$ is the position of the i th particle at time t and $q_i(0)$ is its initial position.

To compute the average diffusion coefficient in the system, we plotted the sum of distance travelled by each particle squared against time. The slope of the curve divided by six times the particle number gives the average diffusion coefficient of the system.

We computed the diffusion coefficient for different state points and plotted it as a function of $\sqrt{T^*}/\rho^*$ and plotted in Fig. 3. The figure shows that, a higher value of λ causes an under estimation of the diffusion coefficient while the lower value of λ gives a better estimation for the same time step.

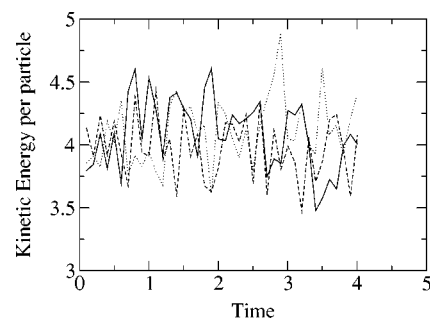


FIG. 2. Kinetic energy per particle variation during simulation with $\lambda=0.05$. The curves and remaining parameters are same as in Fig. 1.

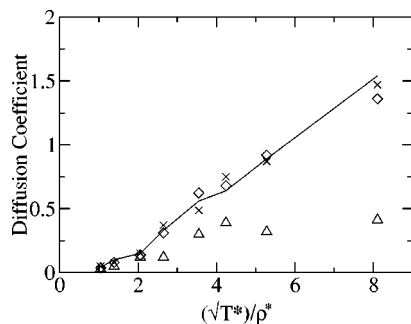


FIG. 3. Diffusion coefficient of a bulk LJ fluid plotted as a function of $(T^*)^{1/2}/\rho^*$ with different values of λ for various state points. The solid line represents the values as given in Table I of Ref. 14. Diamonds are the values of simulation with $\lambda=0.01$ and time step $=10^{-4}$, triangles are simulation results with $\lambda=0.05$ and time step $=10^{-4}$, and crosses are the values obtained with $\lambda=0.01$ and time step $=10^{-5}$, but with stochastic momentum kicks only once every ten steps.

Hence, we decided to select the lower value for λ and shorter time step. As explained above, we reduced the time step by a factor of 10 and at the same time made the momentum kicks less frequent by a factor of 10. Figure 3 shows that such a scheme correctly estimates the diffusion coefficient, as compared with the results reported by Heyes.¹⁴

We also computed the pressure at different densities for two isotherms and the results are plotted in Fig. 4. The pressures calculated here include the tail correction due to long range cut-off used in the calculation of LJ potential. We compared the values of pressure calculated with our scheme, i.e., $\lambda=0.01$ and momenta of the particles getting a random push only once in ten steps, to the standard values reported by Hansen and McDonald.¹⁵ This shows that the stochastic temperature control does not adversely affect equilibrium properties and that it is capable of reaching and maintaining a given state point. To confirm that the equilibrium properties do not depend on the choice of λ , we have also plotted the values of pressure calculated with the higher $\lambda=0.05$.

B. Stochastic chemical potential control

We simulated a system in contact with a reservoir at a fixed chemical potential μ^* and temperature T^* . At every

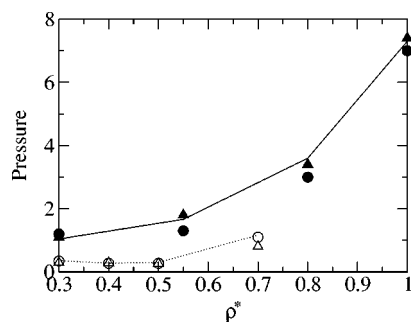


FIG. 4. Pressure plotted as a function of ρ^* for two different temperatures. The solid line indicates the values from Hansen and McDonald (Ref. 15) for temperature 2.74 and the dotted line is for a temperature of 1.35. Circles are computed with $\lambda=0.01$ and triangles are the values with $\lambda=0.05$. The filled symbols are for temperature 2.74 and open symbols for temperature 1.35. A cut-off of 2.5σ has been used.

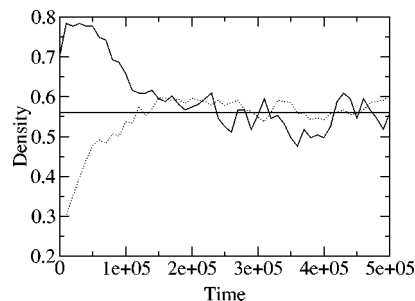


FIG. 5. Density of the system varying with simulation time. In this case, $\mu^* = -16.0$ and $T^* = 1.5$. The solid curve is the simulation of the system that starts with a density 0.7. The dashed curve is the system with a starting density 0.3. The solid line is the density at this state point (0.56) as given by the equation of state of Nicolas (Ref. 16). The potential energy has been cutoff at $r_c = 2.5\sigma$ and a tail correction applied.

step the system tries to gain or lose particles to reach an equilibrium density with the reservoir. The value of ξ^* , the maximum change in ξ which represents the speed with which a particle can shrink or grow, was fixed at 0.1. Acceptance rate at this value is about 35% for creation and deletion. The magnitude of ξ^* controls the speed of equilibration. Too small a value for ξ^* slows down the shrinking or growth and the system needs to run for a long time to reach equilibrium. Too big a value for ξ^* removes the smoothness of the potential energy of the system.

Figure 5 depicts the approach of the system towards equilibrium density. The system consisted of 100 particles placed in a box at $\mu^* = -16.0$ and $T^* = 1.5$. The volume of the box is computed to start it with the desired initial density. We did two different simulations starting the system with a higher and a lower density than the expected equilibrium density. The average equilibrium density of the two simulations is 0.57. The equilibrium density at this state point is 0.56.¹⁶ In both the cases the system tended towards its equilibrium density. Simulations were run for 500 000 runs, and the system equilibrated within the first 100 000 runs. We studied the effect of tail corrections by running separate simulations with and without the tail corrections for two different values of r_c . For a lower cut-off value of 2.5σ without any tail correction the average density for the above system, starting from either higher or lower density was 0.52. However, for the same cut-off, the inclusion of tail correction term improved the average density to 0.57. For a higher cut-off value of 3.5σ the average densities with or without tail correction terms are nearly same (0.56).

The density profiles from the picture show that the density after equilibration is not a constant but fluctuates about an average value. These fluctuations reflect the GC probability distribution, as we would expect.

We ran the simulations till the number of particles remain fairly stable, indicating that the system has reached an equilibrium density for that particular chemical potential. We repeated the calculation of equilibrium density for different chemical potentials and compared the results with those obtained from an equation of state.¹⁶ The results are shown in Fig. 6. From the curve it is evident that the equilibrium density increases with increasing in chemical potential. The

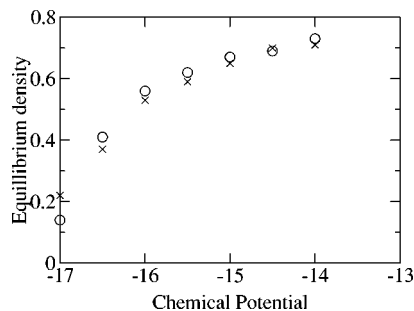


FIG. 6. Equilibrium densities for different chemical potential values. Crosses indicate the values from Nicolas *et al.* (Ref. 16). Circles represent the results of our simulation. The temperature was $T^* = 1.5$, the cut-off was $r_c = 3.5\sigma$, and the tail correction was included.

agreement between the values calculated from our simulation and the values computed using the equation of state confirms the validity of the GCMD method proposed here.

V. CONCLUSIONS

In the stochastic temperature control, too low a value for the maximum momentum change results in rather poor kinetic energy control. But this can be rectified by using a more robust algorithm to solve the Hamilton's equations or by reducing the time step. However, if the momenta of all the particles are getting random kicks at every time step, a reduced time step means too many kicks for the same simulation time. This affects the dynamics of the particles. This can be solved by giving the random kicks to momenta once in a few steps, instead of every time step. Our simulation results with such a scheme agree fairly with the results already available in the literature. The main idea here is to settle for an optimum value of λ while using a simple algorithm at the same time without compromising on the temperature control. Our results demonstrate that such a trade-off can be successfully achieved. We also showed that the stochastic molecular dynamics or the magnitude of the stochastic thermal force reflected by the value of λ does not effect the equilibrium properties.

Besides exploring the influence of the stochastic thermostat on the dynamics of the system, this paper was also concerned with developing and testing a stochastic grand canonical molecular dynamics algorithm. We proposed a trial

conditional probability that although asymmetric for deletions and creations, could be used with a modified Metropolis algorithm to yield a symmetric unconditional transition probability. This guarantees that the classical grand canonical probability distribution is stationary under the present stochastic and deterministic equations of motion, and hence that the time average equals the classical grand canonical system average. We used a fractional particle and partial coupling for its potential energy so that the number of particles in the system was a real number and that the potential energy and pseudopotential were smooth functions that changed continuously as particles were created or destroyed. This enables the algorithm to be used for dense liquids and solids. We tested the algorithm for Lennard-Jones fluids and showed that it yielded results in accord with known literature values. We did not test the effect of the partially coupled solute on the dynamics of the system, although we expect it to be negligible for a sufficiently large system. We expect that for structural information the efficiency of the present GCMD method to be much greater than pure insertion and deletion GCMC, and to be similar to partial coupling GCMC. We believe that the main advantages of the present GCMD algorithm are its ability to yield dynamical information for an open system, and its guarantee that the trajectory is weighted according to the classical grand canonical probability distribution.

¹T. Cagin and B. M. Pettitt, *Mol. Phys.* **72**, 169 (1991).

²C. Lo and B. Palmer, *J. Chem. Phys.* **102**, 925 (1995).

³R. M. Shroll and D. E. Smith, *J. Chem. Phys.* **110**, 8295 (1999).

⁴M. Lupowski and F. van Swol, *J. Chem. Phys.* **95**, 1995 (1991).

⁵A. Papadopoulou, E. D. Becker, M. Lupowski, and F. van Swol, *J. Chem. Phys.* **98**, 4897 (1993).

⁶G. S. Heffelfinger and F. van Swol, *J. Chem. Phys.* **100**, 7548 (1994).

⁷R. F. Cracknell, D. Nicholson, and N. Quirke, *Phys. Rev. Lett.* **74**, 2463 (1995).

⁸P. Attard, *J. Chem. Phys.* **116**, 9616 (2002).

⁹H. C. Anderson, *J. Chem. Phys.* **72**, 2384 (1980).

¹⁰P. Attard (unpublished).

¹¹R. D. Kaminsky, *J. Chem. Phys.* **101**, 4986 (1994).

¹²G. M. Torrie and J. P. Valleau, *Chem. Phys. Lett.* **28**, 578 (1974).

¹³P. Attard, *J. Chem. Phys.* **98**, 2225 (1993).

¹⁴D. M. Heyes, *J. Chem. Soc., Faraday Trans. 2* **79**, 1741 (1983).

¹⁵J. P. Hansen and I. R. McDonald, *Theory of Simple Liquids* (Academic, London, 1986).

¹⁶J. J. Nicolas, K. E. Gubbins, W. B. Streett, and D. J. Tildesley, *Mol. Phys.* **37**, 1429 (1979).